Development and Validation of a New In-Situ Technique to Measure Total Gaseous Chlorine in Air

Teles C. Furlani[1], RenXi Ye[1], Jordan Stewart[1,2], Leigh R. Crilley[1], Peter M. Edwards[2], Tara F. Kahan[3], Cora J. Young[1*]

[1] Department of Chemistry, York University, Toronto, Canada

[2] Department of Chemistry, University of York, York, UK

[3] Department of Chemistry, University of Saskatchewan, Saskatoon, Canada

*Correspondence to: youngcj@yorku.ca

Abstract

Total gaseous chlorine (TCl_g) measurements can improve our understanding of unknown sources of Cl to the atmosphere. Existing techniques for measuring TCl_g have been limited to offline analysis of extracted filters and do not provide suitable temporal information on fast atmospheric process. We describe high time-resolution in-situ measurements of TCl_g by thermolyzing air over a heated platinum (Pt) substrate coupled to a cavity ring-down spectrometer (CRDS). The method relies on the complete decomposition of TCl_g to release Cl atoms that react to form HCl, for which detection by CRDS has previously been shown to be fast and reliable. The method was validated using custom organochlorine permeation devices (PDs) that generated gas-phase dichloromethane (DCM), 1-chlorobutane (CB), and 1,3-dichloropropene (DCP). The optimal conversion temperature and residence time through the high-temperature furnace was 825 °C and 1.5 seconds, respectively. Complete conversion was observed for six organochlorine compounds, including alkyl, allyl, and aryl C-Cl bonds, which are amongst the strongest Cl-containing bonds. The quantitative conversion of these strong C-Cl bonds suggests complete conversion of similar or

weaker bonds that characterize all other TCl_g. We applied this technique to both outdoor and indoor environments and found reasonable agreements in ambient background mixing ratios with the sum of expected HCl from known long-lived Cl species. We measured the converted TCl_g in an indoor environment during cleaning activities and observed varying levels of TCl_g comparable to previous studies. The method validated here is capable of measuring in-situ TCl_g and has a broad range of potential applications.

1. Introduction

Chlorine (Cl) containing compounds in the atmosphere can impact air quality, climate, and health (Saiz-Lopez and Von Glasow, 2012; Simpson et al., 2015; Massin et al., 1998; White and Martin, 2010). Gaseous chlorinated compounds are either organic (e.g., dichloromethane, chloroform, and carbon tetrachloride) or inorganic (e.g., Cl_2, HCl, and $ClNO_2$), with inorganic Cl being more reactive under most atmospheric conditions. In this work, total gaseous Cl (TCl_g) refers to all gas-phase Cl-containing species weighted to their Cl content, including both inorganic and organic species. While groups of chlorinated species are often considered based on reactivity considerations (e.g., reactive chlorine, Cl_y), TCl_g includes all molecules that contain one or more Cl atoms:

$$TCl_g = 4*[CCl_4] + 3*[CHCl_3] + 2*[CH_2Cl_2] + [CH_3Cl] + 2*[Cl_2] + [HOCl] + \ldots\ldots \quad \text{E1}$$

Impacts on air quality and climate are due to the high reactivity of atomic Cl produced by common atmospheric reactions (e.g., photolysis and oxidation) of Cl-containing compounds (Riedel et al., 2014; Sherwen et al., 2016; Haskins et al., 2018). The Cl cycle is important to atmospheric composition in the stratosphere and troposphere, affecting species including methane, ozone, and particles (both formation and composition), which influence air quality and climate (Solomon, 1999; Riedel et al., 2014; Young et al., 2014; Sherwen et al., 2016). High levels of some TCl_g

species (e.g., Cl_2 and carbon tetrachloride) are known to be toxic (White and Martin, 2010; Unsal et al., 2021). The implications of many TCl_g species on human health are not well understood for low level exposure for extended periods of time. Potential health impacts of organic chlorinated compounds include hepatotoxicity, nephrotoxicity, and genotoxicity (Unsal et al., 2021; Henschler, 1994). Impacts of inorganic chlorinated species include the chlorination of squalene, a major part of human skin oils, by HOCl (Schwartz-Narbonne et al., 2019); respiratory irritation and airway obstruction by Cl_2 (White and Martin, 2010); and increased incidence of asthma and other chronic respiratory issues following exposure to chloramines (Massin et al., 1998).

Sources of Cl to the atmosphere are highly variable and depend on both direct emissions and indirect regional Cl activation chemistry (Finlayson-Pitts, 1993; Raff et al., 2009; Khalil et al., 1999). Direct emissions of TCl_g can come from numerous natural and anthropogenic activities such as, but not limited to, ocean and volcanic emissions, biomass burning, disinfection (i.e., household cleaning, pool emission, etc), use of solvents and heat transfer coolants, and incineration of chlorinated wastes (Blankenship et al., 1994; Lobert et al., 1999; Keene et al., 1999; Butz et al., 2017; Wong et al., 2017; Fernando et al., 2014). Activation of Cl is another source, occurring when atmospheric processes transform relatively unreactive chloride (Cl^-, such as sea salt, NaCl) into reactive gaseous chlorine (Cl_y), which will contribute to TCl_g. Understanding global levels of TCl_g is difficult due to complex emissions and chemistry. Our best estimates come from modelling studies combined with collaborative efforts to compose policy reports on halogenated substances, such as the World Meteorological Organization (WMO) Scientific Assessment of Stratospheric Ozone Depletion (WMO (World Meteorological Organization), 2018). Mixing ratio estimates of halogenated species from this report are summed from individual measurements (e.g., National Oceanic and Atmospheric Administration (NOAA) and Advanced Global Atmospheric Gases

Experiment (AGAGE)). The WMO report includes flask (captured gas from clean air sectors) and in-situ measurements from field campaigns and routine sampling sites (e.g., CONvective Transport of Active Species in the Tropics (CONTRAST)) (Prinn et al., 2018; Pan et al., 2017; Andrews et al., 2016; Montzka et al., 2021; Adcock et al., 2018). In the most recent WMO report (2018), a decrease of 12.7 ± 0.9 pptv Cl yr^{-1} in total tropospheric Cl was determined for Montreal Protocol-controlled substances (e.g., chlorofluorocarbons (CFCs) and hydrochlorofluorocarbons (HCFCs)). The decrease in Montreal Protocol-controlled emissions has been slightly offset by an increase in relatively short-lived substances (e.g., dichloromethane) that are not controlled by the Montreal Protocol (WMO (World Meteorological Organization), 2018). Despite the emissions of these regulated chlorinated species being relatively well-constrained, new sources for some of these compounds have appeared in the recent past. For example, unexpected increases observed in CFC-11 emissions suggested new unreported production (WMO (World Meteorological Organization), 2018). A new source of chloroform was also recently identified and attributed to halide containing organic matter derived from penguin excrement in the Antarctic tundra (Zhang et al., 2021). Atmospheric levels of TCl_g will additionally be impacted by emission sources that are relatively poorly constrained, including combustion and disinfection. Increasing levels of chlorinated species from known and unknown pathways was observed in a recent ice core study, which estimated an increase of up to 170% of Cl_y (= BrCl + HCl + Cl + ClO + HOCl + $ClNO_3$ + $ClNO_2$ + ClOO + OClO + 2·Cl_2 + 2·Cl_2O_2 + ICl) from preindustrial times to the 1970s could be attributed to mostly anthropogenic sources (Zhai et al., 2021).

Understanding TCl_g source and sink chemistry is not only important for the ambient atmosphere but also for indoor environments. Uncertainty in sources and levels of chemicals, including Cl-containing compounds, indoors is related to heterogeneity in sources and individual

indoor environments, and the fact that relatively few studies have focused on indoor chemistry compared to outdoor. The role of chlorinated species on indoor air quality has been investigated in a few studies (Mattila et al., 2020; Wong et al., 2017; Dawe et al., 2019; Giardino and Andelman, 1996; Shepherd et al., 1996; Doucette et al., 2018; Nuckols et al., 2005). Most studies have focused on cleaning with Cl-based cleaners, in which HOCl and other inorganic compounds have been observed in the gas phase at high levels (Wong et al., 2017; Wang et al., 2019; Mattila et al., 2020). Some studies have reported the presence of organic chlorinated species such as chloroform and carbon tetrachloride above bleach cleaning solutions indoors (Odabasi, 2008; Odabasi et al., 2014), and chloroform has been observed during water-based cleaning activities, such as showering and clothing washing (Nuckols et al., 2005; Shepherd et al., 1996; Giardino and Andelman, 1996).

Constraining the Cl budget is critical to better understanding its contributions to climate, air quality, and human health. Robust total Cl measurements are useful because it is not always feasible to routinely deploy individual measurements of the large number of known Cl-containing compounds (Table S1). As described above, estimates of TCl_g from models and summed measurements have demonstrated gaps in our knowledge. It is therefore essential to have a method capable of measuring true TCl_g to explain discrepancies between model and measured estimates due to unknown species. Measurements of total elemental composition in the condensed phase, including total Cl, have been used for monitoring and managing both known and unknown compounds (Miyake et al., 2007c, a; Yeung et al., 2008; Miyake et al., 2007b; Kannan et al., 1999; Xu et al., 2003; Kawano et al., 2007). However, TCl_g methods have been limited to offline analysis of scrubbed sample gas (e.g., flue); these methods rely on multiple extraction steps and the application of condensed-phase total Cl analyses, such as combustion ion chromatography (Miyake et al., 2007a; Kato et al., 2000) or neutron activation analysis (Berg et al., 1980; Xu et al.,

2006, 2007). Because offline techniques suffer from extraction uncertainties and do not have the temporal resolution to effectively probe fast chemistry in the atmosphere, in-situ measurements of total elemental gaseous composition have been developed for several elements (Hardy and Knarr, 1982; Veres et al., 2010; Roberts et al., 1998; Maris et al., 2003; Yang and Fleming, 2019). For example, total nitrogen has been measured using Pt-catalyzed thermolysis coupled to online chemiluminescence detection (Stockwell et al., 2018). Using a similar approach, we describe here a method for TCl_g, where catalyzed thermolysis is coupled to a high time-resolution HCl cavity ring-down spectrometer (CRDS). This technique relies on the complete thermolysis of TCl_g, which yields chlorine atoms. These Cl atoms readily form HCl via hydrogen abstraction (R1), in this case from propane (or its thermolysis products) that is supplied in excess.

$$Cl\ (g) + C_3H_8\ (g) \rightarrow HCl\ (g) + C_3H_7\ (g) \qquad R1$$

The objectives of this paper are to: (i) Develop and validate an instrument capable of in-situ measurement of TCl_g through conversion to HCl and detection by CRDS; and (ii) demonstrate application of the technique to outdoor and indoor TCl_g measurements.

2. Materials and experimental methods

2.1. Chemicals

Commercially available reagents were purchased from Sigma-Aldrich (Oakville, Ontario, Canada): dichloromethane (DCM, HPLC grade), 1-chlorobutane (CB, 99.5%), cis-1,3-dichloropropene (DCP, 97%), trichlorobenzene (TrCB, 99%), tetrachlorobenzene (TeCB, 98%), pentachlorobenzene (PeCB, 96 %), sodium chloride, and 52 mesh sized platinum catalyst (99.9 %). Toluene (HPLC grade) was purchased from BDH VWR (Mississauga, Ontario, Canada). Nitrogen (grade 4.8) and propane (C_3H_8, 12.7% in nitrogen, v/v) gas was from Praxair (Toronto, Ontario, Canada). Experiments used deionized water generated by a Barnstead Infinity Ultrapure Water System (Thermo Fisher Scientific, Waltham, Massachusetts, USA; 18.2 MΩ cm^{-1}). A

permeation device (PD) described previously was used to generate gaseous HCl (Furlani et al., 2021). Chlorine-free zero air was generated by a custom-made zero-air generator.

2.2. HCl and total chlorine (HCl-TCl) instrument

The main components of the HCl-TCl (Figure 1) are platinum catalyst mesh, a quartz glass flow tube, a split-tube furnace (Protégé Compact, 1100°C max temperature, Thermcraft incorporated, North Carolina, USA), and a CRDS HCl analyzer (Picarro G2108 Hydrogen Chloride Gas Analyzer). The platinum catalyst consisted of ~2 g platinum mesh with a total combined surface area of 134 cm^2. Sample gas was mixed with critical orifice-regulated (Lenox laser, Glen Arm, Maryland, USA, 30 psi; SS-4-VCR-2-50) propane gas (62 ± 6 standard cubic centimetres per minute (sccm)), provided in excess prior to introduction to the furnace to promote (R1). The added propane does not fully thermolyze at temperatures < 650 °C, which can lead to spectral interferences in the CRDS analyzer (Figure S1) and should only be added when temperatures exceed 650°C (Furlani et al., 2021). All lines and fittings were made of perfluoroalkoxy (PFA) unless stated otherwise. The mixing line carrying clean air dilution flows was controlled by a 10 L min^{-1} mass flow controller (MFC, GM50A, MKS instruments, Andover, Massachusetts, USA). The length of the sample gas tubing to the furnace was 0.6 m, and the transfer line between the furnace and CRDS was 0.2 m. The furnace transfer line met an overflow tee when delivering flows greater than the CRDS flowrate of 2 L min^{-1}. The coupled CRDS can capture transient fast HCl formation processes on the timescale of a few minutes, limited by the high adsorption activity of HCl on inlet surfaces (discussed further in Section 3.3). The CRDS collects data at 0.5 Hz. Limits of detection (LODs) for the CRDS were calculated as three times the Allan–Werle deviation in raw signal intensity when overflowing the inlet with zero air directed

into the CRDS for ~ 10 h. The 30-sec LOD is 18 pptv and well below expected HCl from TCl_g conversion (Furlani et al., 2021a).

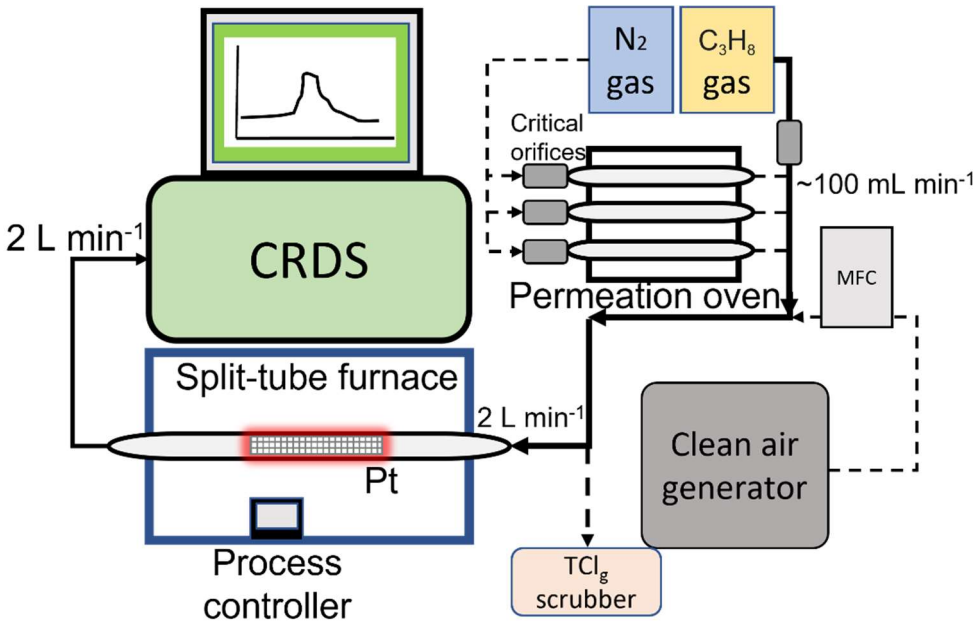

Figure 1. Sampling schematic showing the key components of the HCl-TCl coupled to the CRDS analyzer. Dashed lines indicate parts of the apparatus used only during validation. Not to scale.

2.3. Preparation of organochlorine permeation devices (PDs)

Organochlorine PDs were prepared as follows: approximately 200 µL of DCM, CB, or DCP was pipetted into a 50 mm PFA tube (3 mm i.d. with 1 mm thickness), thermally sealed at one end and plugged at the other end with porous polytetrafluoroethylene (PTFE) (13 mm length by 3.17 mm o.d.). The polymers allow a consistent mass of standard gas to permeate at a given temperature and pressure. The method for temperature and flow control of the PDs is described in detail in Lao et al. (2020). Briefly, an aluminum block that was temperature-controlled (Omega™; CN 7823, Saint-Eustache, QC, Canada) using a cartridge heater (Omega™; CIR-2081/120V, Saint-Eustache, QC, Canada) housed the PD and was regulated to 30.0 ± 0.1 °C. Dry N_2 gas flowed through a PFA housing tube (1.27 cm o.d.) in the block that contained the PD. Stable flows of carrier gases passed through the housing tube in the oven were achieved using a 50 µm diameter critical orifice (Lenox

laser, Glen Arm, Maryland, USA, 30 psi; SS-4-VCR-2-50) and were 120 ± 12, 99 ± 9.9 and 120 ± 12 sccm for DCM, CB, and DCP, respectively. Flows were measured using a DryCal Definer 220 (Mesa Labs, Lakewood, Colorado, USA). The mass emission rate of each organochlorine from the PDs was quantified gravimetrically over a period of approximately 4 weeks (mass accuracy ± 0.001 g). Mass emission rates for each PD were determined as 640 ± 10, 240 ± 40, and 1.20×10^4 ± 0.02×10^4 ng min^{-1} (n=3, ± 1σ) at 30 °C for DCM, CB, and DCP, respectively.

2.4. HCl-TCl optimization

Gas phase standards of DCM, CB, and DCP were used to test the conversion efficiency of chlorinated compounds to form HCl. Bond dissociation energies for carbon-Cl bonds typically range between 310 and 410 kJ mol^{-1} (Tables S1, S2). The split-tube furnace has a process controller capable of increasing or decreasing temperature at a set °C min^{-1}, which allowed us to identify the temperature at which enough energy was provided to break the bonds. By introducing a consistent amount of each of the organochlorines, separately, to the HCl-TCl set over a simple temperature ramping program we could monitor in real-time the conditions necessary to break the bonds by measuring the formation of the resulting HCl. The operating temperature was determined when complete conversion of the measured TCl_g for the tested compounds was sustained at 100% conversion based on PD emission rates.

To determine the optimal residence time in the quartz tube with the Pt catalyst, flows of 0.6–5.5 L min^{-1} containing DCM sample gas in clean air were tested yielding a range of residence times between 0.5 and 4.5 sec in the furnace. Temperature remained constant at 825 °C throughout the experiment, and a dilution flow of 4.0 L min^{-1} of clean air was added to the sample flow exiting the furnace before introduction to the CRDS.

We tested the HCl transmission of the HCl-TCl at 2 mixing ratios (18 and 10 ppbv) using a 12 M HCl PD with zero air dilution flows of 3.5 or 5 L min^{-1} using a 5 L min^{-1} MFC (GM50A, MKS instruments, Andover, Massachusetts, USA). The HCl recovery through the furnace was tested by comparing measured HCl mixing ratios through HCl-TCl to those with the furnace flow tube replaced by a similar length of tubing. A heat gun (Master Varitemp® vt-750c) was used to heat the flow tube entrance to ~80 °C to minimize HCl sorption. We tested the HCl-TCl conversion efficiency for 5 different mixing ratios of three organochlorine PD standards (DCM, CB, and DCP) under three conditions: (1) both Pt catalyst and added propane, (2) only Pt catalyst, and (3) only added propane. Each gas was tested individually under the same conditions; sample gas from PDs was mixed with propane and immediately diluted into clean air using a 10 L min^{-1} MFC. The dilution flows ranged from 2.2–9.0 L min^{-1}. The sampling lines were the same lengths as stated previously. In this experiment, the CRDS flowrate of 2 L min^{-1} was sufficient to give an optimal residence time of 1.5 sec through the HCl-TCl (see Section 3.1). In all experiments the CRDS subsampled through the furnace from the main transfer line and the excess gas was directed outdoors through a waste line containing a carbon trap (Purakol, Purafil, Inc, Doraville, Georgia, USA). We also tested the HCl-TCl conversion efficiency for two different quantities of three chlorobenzenes (TrCB, TeCB, and PeCB). Due to their high boiling points, PDs of these compounds could not be prepared. Instead, small volumes of approximately 1 mM solutions of these compounds dissolved in toluene were directly introduced to the HCl-TCl while it was sampling room air. Room air measurements of TCl_g were consistently >1 ppbv. These were measured before each experiment and did not affect the peak integration described below. With a short piece of tubing used as an inlet, 1 and 2 μL of each compound was injected onto the inner surface of the tubing, which was heated to ~100 °C with a heat gun to facilitate volatilization. The

resulting signals were integrated over a time period of 2.5 hours to obtain the total quantity of HCl detected by the CRDS, which was used to calculate conversion efficiency. To account for uncertainties in peak integration, a high and low peak area boundary was determined, with the average peak area taken for each injection. Duplicates of each injected quantity were performed, except for 1 µL TrCB, which was performed in triplicate.

To determine if there was any positive bias in the TCl_g, measurement from the conversion of particulate chloride (pCl^-), NaCl aerosols were generated by flowing 2 L min^{-1} of chlorine free zero air through a nebulizer containing a solution of 2% w/w NaCl in deionized water. The aerosol flow was then mixed with 1 L min^{-1} of chlorine free dry zero air to achieve a total flow of 3 L min^{-1}, The HCl-TCl (2 L min^{-1}) then sampled off this main mixing line. Chloride was added after monitoring background zero air levels. After ~3 hours of measuring the converted pCl^-, a PTFE filter (2 µm pore size, 47 mm diameter, TISCH scientific, North Bend, Ohio, USA) was added inline onto the inlet of the HCl-TCl.

2.5. Outdoor air HCl-TCl measurements

Outdoor air sampling was performed between 00:00 on July 7 to 20:00 on July 11, 2022 (Eastern daylight time, EDT). The sampling site was the air quality research station located on the roof of the Petrie Science and Engineering building at York University in Toronto, Ontario, Canada (43.7738° N, 79.5071° W, 220 m above sea level). The HCl-TCl was co-located with a Campbell Scientific weather station paired with a cr300 datalogger. All inlet lines and fittings were made of PFA unless stated otherwise. All indoor inlet lines and fittings were kept at room temperature. A mass flow controller (GM50A, MKS instruments, Andover, Massachusetts, USA) regulated a sampling flow of 14.7 L min^{-1} using a diaphragm pump through a 2.4 m sampling inlet (I.D. of 0.375") from outdoors. The outdoor air was pulled through a 2.5 µm particulate matter

247 cut-off URG Teflon Coated Aluminum Cyclone (URG Corporation, Chapel Hill, North Carolina,
248 USA) to remove larger particles and then passed through a PTFE filter (2 μm pore size, 47 mm
249 diameter, TISCH scientific, North Bend, Ohio, USA). The CRDS subsampled 2 L min^{-1} through
250 the furnace off the main inlet line, yielding a total inlet flow of 16.7 L min^{-1}. The apparatus had
251 zero air overflow the inlet 1 hour prior to and after outdoor sampling. The CRDS sample flow
252 passed first through a PTFE filter (2 μm pore size, 47 mm diameter) and then two high efficiency
253 particulate air (HEPA) filters contained within the CRDS outer cavity metal compartment heat-
254 regulated to 45 °C. Instances of flagged instrument errors in the CRDS data during ambient
255 observations were removed as standard practice in quality control procedures. The dataset can be
256 found in Furlani et al., (2022).

257 **2.6. Indoor air HCl-TCl and HOCl analyzer measurements**

258 To test indoor applications of the HCl-TCl, a 1 m^2 area of laboratory floor was cleaned with
259 a commercial spray bottle cleaner (1.84 % sodium hypochlorite w/w) and emissions were
260 compared with an HOCl analyzer. The HOCl analyzer is a commercial instrument designed to
261 quantify gaseous hydrogen peroxide (H_2O_2) using CRDS (Picarro PI2114 Hydrogen Peroxide
262 Analyzer; Picarro Inc.). The instrument is also sensitive to HOCl due to similar absorbance
263 wavelengths of their first overtone stretches in the near IR. The wavelengths monitored have been
264 altered to selectively detect HOCl. Details on instrument calibration and validation are provided
265 in Stubbs et al. (2022).

266 The distance from the suspended 2 m inlet lines of both instruments to the floor was ~1 m.
267 The flowrate through the furnace and inlet was the 2 L min^{-1} CRDS flowrate. The flowrate for the
268 HOCl analyzer was 1 L min^{-1}. The sectioned off area was cleaned four times, spraying 32 times
269 for each application using the commercial cleaner. Three of these events were measured using the

HCl-TCl and HOCl analyzer, while one event was measured using the HCl CRDS only. The dataset can be found in Furlani et al., (2022).

3. Results and Discussion

3.1. HCl-TCl temperature and residence time optimization

We validated this method by testing conversion efficiency of organochlorines under different operating parameters and conditions. Testing all TCl_g species is not feasible, but by testing compounds that contain strong Cl-containing bonds, we infer at least equal efficacy of the system in the breakage of relatively weaker Cl-containing bonds (Tables S1 and S2). We selected strong Cl-containing bonds (i.e., alkyl, allyl, and aryl chlorides) and used them as a proxy for compounds containing weaker Cl bonds; therefore, by demonstrating their complete conversion we set precedent for conversion of all TCl_g. The temperature of the furnace is a key factor in accomplishing complete thermolysis, and the minimum temperature of the furnace containing the Pt catalyst to break the C-Cl bonds in DCM was determined. A simple temperature ramping program was used to determine the breakthrough temperature. The temperature was increased at a rate of 2.7 °C min^{-1} starting at 300 °C and ending at 800 °C. The temperature breakthrough was observed when complete conversion of the expected HCl for the tested compounds (based on PD emission rate) was stable after reaching the optimal temperature. It was found to be ~800 °C for the tested organochlorines (Figure S2).

Determining the optimal residence time of sample gas in the HCl-TCl is also essential for an optimized TCl_g conversion method. Using a temperature slightly above the observed breakthrough temperature of 800 °C determined above (825 °C), six residence times were tested with DCM, ranging from 0.5 to 4.5 seconds in the HCl-TCl (Figure 2). At each residence time the conversion efficiency was determined, where conversion efficiency was calculated as follows:

293 $$\text{Conversion efficiency} = \frac{\text{Measured TCl}_g}{\text{Expected TCl}_g} \times 100\ \% \qquad \text{E2}$$

294 The optimal residence time was ~1.5 seconds, corresponding to a conversion efficiency of 100.1
295 ± 0.1 %. The uncertainty in conversion efficiency measurements is the variability in the measured
296 HCl signal for 30 minutes after a signal plateau was observed. The reported uncertainty does not
297 include uncertainties in mixing, or turbulence induced surface effects, which we cannot quantify.
298 When residence times were lower (i.e., sample gas traveled more quickly through the system) than
299 1.5 seconds, the conversion efficiencies were lower by 2 – 10 %, the measured HCl signal was
300 more erratic, and it took longer to stabilize. When residence times were higher (i.e., sample gas
301 traveled more slowly through the system) than 1.5 seconds, the conversion efficiencies were
302 comparable (± 2 %), but the measured HCl suffered from longer equilibration times (~30 minutes,
303 more than double the 1.5 residence time) and therefore a slower response time, likely due to
304 increased surface effects of HCl after exiting the furnace. An optimal residence time of 1.5 seconds
305 was selected for all HCl-TCl experiments for its good conversion efficiency and reasonable
306 response time (see Table S3).

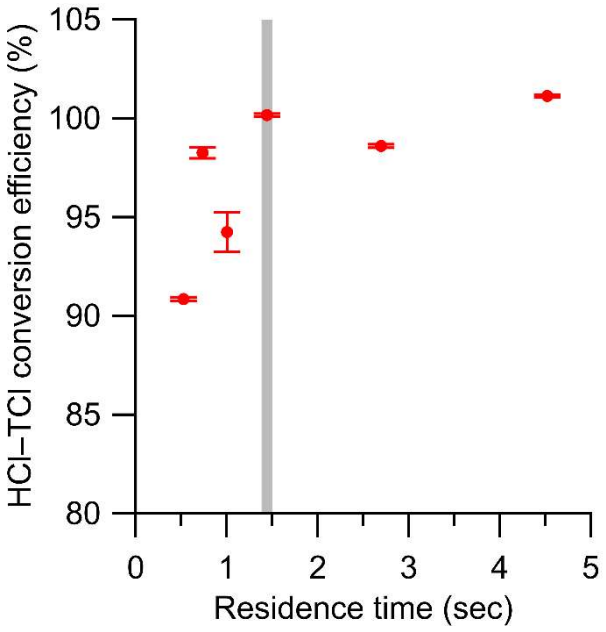

Figure 2. Conversion efficiency of DCM plotted against residence time in the HCl-TCl at 825 °C. Error bars represent the percent relative standard deviation of the measured HCl by the CRDS over ~30 minutes, after signal has plateaued. Grey vertical line denotes the selected residence time. Note that the error bars are represented by the precision of the instrument, and we expect there would be greater experiment-to-experiment variability.

3.2. HCl-TCl conversion efficiency

The efficiency of HCl throughput in the HCl-TCl was tested. Initial tests resulted in transmission efficiencies of 81.2% ± 1.4 (n = 3) and 88.1% (n = 1) for 18 ppbv and 10 ppbv HCl, respectively. At the inlet to the furnace, a small piece of the quartz tube is not heated. We hypothesized that complete transmission of HCl was hindered through sorption to that portion of quartz tube. Repeating the experiment with heat applied led to increased throughput efficiencies of 85.7% (18 ppbv, n = 1) and 93.9% (10 ppbv, n = 1). Therefore, good HCl throughput efficiency was demonstrated overall, with the cause of minor HCl losses identified to be sorption losses to room temperature glass. Conversion of particulate chloride (pCl^-) was observed to take place in the HCl-TCl (Figure S3), but once a filter was introduced the signal returned to background levels. Thus, to capture only gaseous TCl_g from samples that may contain particulate chloride, a

particulate filter should be used. Use of a filter could introduce blow on (i.e., partitioning of semi-volatile species) and/or blow off (i.e., processing of particulate chloride) artifacts. We have previously shown that HCl—likely to be the most surface-active component of TCl_g—is not greatly impacted by the presence of filters (Furlani et al., 2021), indicating blow on effects are likely minimal. However, the extent to which blow on effects should be considered will depend on the composition of the TCl_g mixture and the temperature. Blow off effects will depend on ambient particulate chloride levels and can be mitigated by regularly changing the filter to prevent significant particulate chloride accumulation.

The conversion efficiency of each of the two alkyl chlorine and one allyl chlorine compounds using the HCl-TCl was tested at 5 different mixing ratios. See Table S4 for summary of mixing ratios used; all lower mixing ratios were generated by diluting the highest mixing ratio of each compound by chlorine-free zero air. All three showed good linearity and near 1:1 correlation with the HCl expected to be formed from the PD under standard operating conditions (Figure 3). Due to differences in PD emission rates, the values in Figure 3 are normalized to the highest mixing ratio to visualize comparisons more easily. With both Pt and propane the HCl-TCl conversion was 99.6 ± 3.2, 104.8 ± 5.6, and 102.7 ± 7.8% for DCM, CB, and DCP, respectively (Table 1), as the average conversion efficiency ± relative standard deviation. From Figure 3 the comparison between expected and measured TCl_g is illustrated by near unity in the orthogonal distance regression slope (±1σ, the error in the regression analysis), and was 0.996 ± 0.012, 1.048 ± 0.060, and 1.027 ± 0.061 for DCM, CB, and DCP, respectively. With only the Pt catalyst, the HCl-TCl conversion was 80.7 ± 0.4, 54.1 ± 1.6, and 54.3 ± 3.5% for DCM, CB, and DCP, respectively (Figure S4, Table 1). This result indicates the added hydrogen source (propane) is needed to promote R1. Although necessary in this laboratory scenario, some ambient conditions may be rich

enough in hydrogen-containing molecules that excess propane is not needed. However, providing propane in excess ensures the presence of an abundance of hydrogen atoms that can be readily abstracted by Cl atoms via R1. When the Pt catalyst was removed, the HCl-TCl conversion was 94.4 ± 4.6, 44.2 ± 0.9, and 41.7 ± 3.4% for DCM, CB, and DCP, respectively (Figure S4, Table 1). The observed dependence of the Pt catalyst indicates that a reactive surface is important

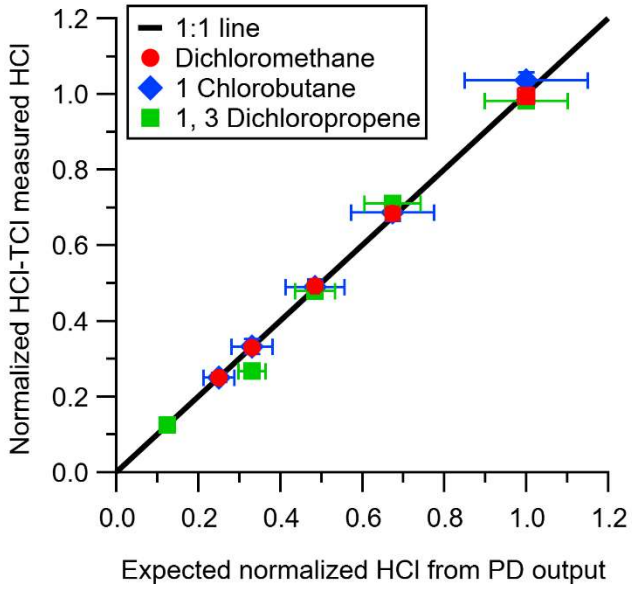

Figure 3. HCl measured by CRDS plotted against the expected HCl from HCl-TCl converted DCM (red circle), 1-chlorobutane (blue diamond), and 1,3-dichloropropene (green square) under condition (1). All values are normalized to the highest expected HCl concentration to better illustrate deviations from unity (black line). Error bars on the y-axis represent 1σ in the HCl signal over 10 minutes. Error bars on the x-axis represent the uncertainty in the PD used to generate DCM.

Table 1. Conversion efficiency for tested Cl-containing compounds under different conditions (both Pt and propane; Pt only; propane only). Note that chlorobenzenes were only tested under Pt and propane conditions.

Tested TCl_g species	Cl bond dissociation energy (kJ mol^{-1})	Conversion efficiency (%)		
		Pt and propane	Pt only	Propane only
Dichloromethane (DCM)[a]	310	99.6 ± 3.2	80.7 ± 2.4	94.4 ± 6.6
1-Chlorobutane (CB)[a]	410	104.8 ± 5.6	54.1 ± 6.6	44.2 ± 5.9
1, 3-Dichloropropene (DCP)[a]	350	102.7 ± 7.8	54.3 ± 5.2	41.7 ± 5.1

Trichlorobenzene (TrCB)[b]	400	97.0 ± 19.9		
Tetrachlorobenzene (TeCB)[b]	400	90.6 ± 10.3		
Pentachlorobenzene (PeCB)[b]	400	90.2 ± 14.8		

[a]Conversion efficiency was determined from the orthogonal distance regression slope and ± σ and propagated error from individual permeation devices.
[b]Conversion efficiency was determined directly by the quantity (mol) of HCl measured from liquid injections of 1 mM standards. The error represents ±σ of measurements for n = 5 (TrCB) or n = 4 (TeCB, PeCB) injections.

to achieve complete thermolysis at 825 °C. The relatively higher conversion for DCM in the absence of the Pt catalyst or hydrogen source may be attributed to its lower bond dissociation energy (310 kJ mol^{-1}) compared to estimated bond dissociation energies for CB and DCP (CB inferred from Table S2 (~410 kJ mol^{-1}), and DCP from tetrachloroethylene (350 kJ mol^{-1} in Table S1)). It is possible that a higher temperature could lead to full conversion of TCl_g in the absence of Pt catalyst; however, that was not explored in this study. To further validate the HCl-TCl, the conversion efficiency of three aryl chlorine compounds were tested under the final operating conditions (i.e., in the presence of both Pt and added propane). The TCl_g measured from the three aryl compounds was unity, within the uncertainty of the measurement (Table 1).

The results for all six compounds show that the HCl-TCl is capable of complete conversion of mono and polychlorinated species on sp^3 and sp^2 carbons using the determined temperature and flow conditions. The complete thermolysis of the strongest C-Cl bond on the primary alkyl chloride (CB) demonstrates the efficacy of the HCl-TCl. Breaking these relatively strong C-Cl bonds, with consistent conversion efficiency across alkyl, allyl, and aryl C-Cl bonds, is a good proof of concept for complete conversion of all bonds of similar or weaker bond energies that characterize all other TCl_g. To practically validate the HCl-TCl under real-world conditions with atmospherically relevant TCl_g mixtures and mixing ratios we also deployed and configured the system to measure outdoor and indoor air.

3.3. Performance metrics of HCl-TCl

Using a flow of zero air through the HCl-TCl, method limits of detection (LODs) were calculated as three times the Allan-Werle deviation (Figure 4) when overflowing a 20 cm inlet (3.17 mm i.d.) with zero air for one hour. The LODs determined in the measurements for 2 second, 1 minute, 5 minute, and 1 hour integration times were 73, 15, 10, and 8 pptv, respectively. The response time of the instrument was assessed during experiments with DCM, CB, and CP. The time for the signal to decay after removal of the PDs was determined to 37 % (1/e) and 90 % (t_{90}) of the maximum signal. The maximum time to achieve 1/e was 23 seconds, while the maximum time to achieve t_{90} was 189 seconds (Table S3). These are comparable to the response times for the HCl CRDS instrument itself (Furlani et al., 2021), suggesting the addition of the inlet furnace has a modest impact on the residence time. Given the high mixing ratios used to test the response times, we argue that under most conditions relevant to indoor and outdoor atmospheric chemistry, a sample integration time of one minute will minimize any time response effects. Data for outdoor and indoor sampling described in Sections 3.4 and 3.5 were therefore averaged to one minute. During all experiments with gaseous reagents, no evidence of catalyst performance degradation was observed.

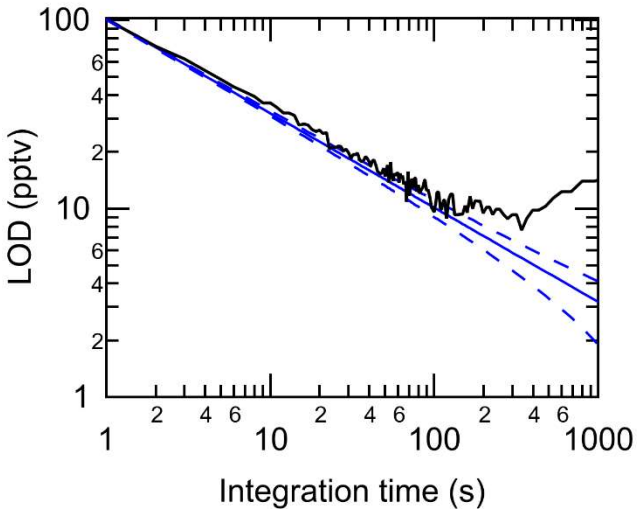

Figure 4. Allan-Werle deviation (3σ) in the HCl-TCl purged with zero-air (black line) shown with the ideal deviation (no drift, solid blue line) and associated error in the deviation (dashed blue line).

3.4. HCl-TCl applications to outdoor air

We deployed the system to measure ambient outdoor air, which we compare to the expected TCl_g range from complete thermolysis of previously measured Cl-containing compounds, estimated to be between 3.3 and 19 ppbv (Table S1). Global background levels of long-lived chlorine-containing species ($LLCl_g$) are well established (WMO (World Meteorological Organization), 2018) and were calculated by equation 3 using data from Table S1:

$$LLCl_g = 3*[CCl_3F] + 2*[CCl_2F_2] + 4*[CCl_2FCCl_2F] + 4*[CCl_3CClF_2] + 3*[CCl_3CF_3] + 2*[CClF_2CClF_2] + 2*[CCl_2FCF_3] + [CClF_2CF_3] + [CHClF_2] + [CH_2ClCF_3] + 2*[CH_3CCl_2F] + [CBrClF_2] + 4*[CCl_4] \quad E3$$

A global background for $LLCl_g$ of approximately 2.6 ppbv is expected ((WMO (World Meteorological Organization), 2018), Table S1). The maximum, minimum, and median of observed ambient TCl_g were 536.3, 2.0, and 3.1 ppbv, respectively (Figure 5). Measurements of HCl alone were not made during these periods but reported ranges of HCl mixing ratios for this sampling location from Furlani et al. (2021) and Angelucci et al. (2021) were typically below 110 pptv, with intermittent events up to 600 pptv. The filter present in the inlet was unlikely to have led to artifacts in this measurement. Particulate chloride is negligible in continental summertime environments (Kolesar et al., 2018), indicating blow off artifacts would be minimal. Most ambient TCl_g measurements were above the expected mixing ratio of $LLCl_g$. It is possible that semi-volatile chlorinated species could have partitioned to the filter, acting as a blow on effect, and leading to an underestimate of TCl_g. However, the warm temperatures during sampling (13 to 31 °C) and high observed TCl_g levels suggest this was not a large effect. There is clear evidence of TCl_g sources beyond $LLCl_g$ at the sampling site, with several plumes of elevated TCl_g intercepted. For example, the maximum TCl_g measurement (536.3 ppbv) was made in a plume just after noon on

July 7. Another plume was detected on July 11, with a maximum TCl_g of 42.1 ppbv. Though the purpose of this study was not to determine sources of TCl_g, we observed that plumes containing elevated TCl_g arrived from the S-SW of the sampling site, where several facilities that had reported tens to thousands of kg of yearly emissions to air of Cl-containing species are located (Figure S5).

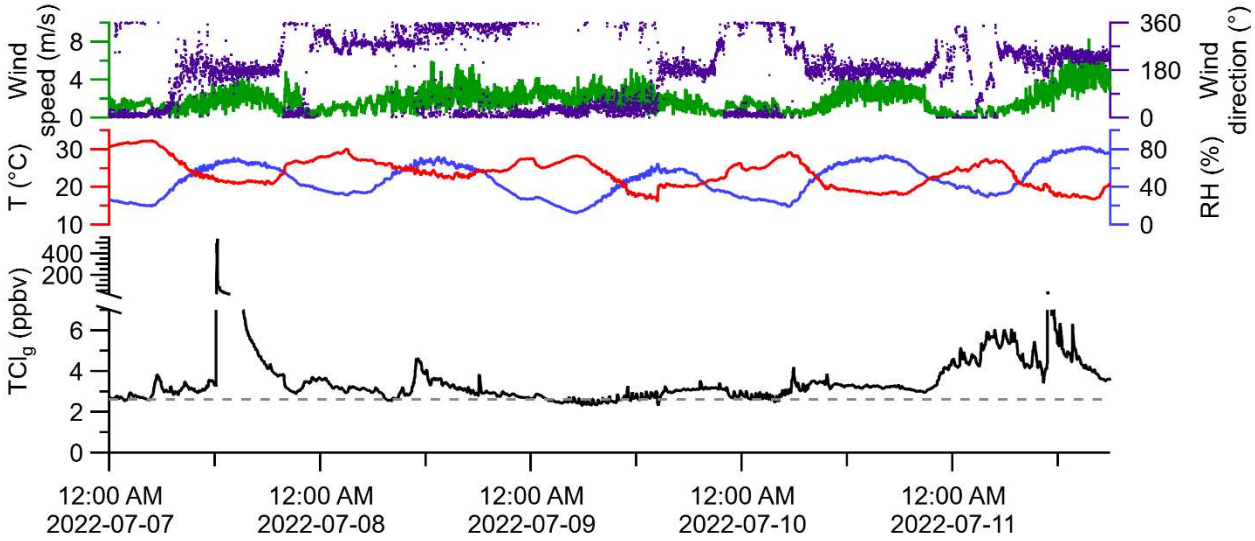

Figure 5. Monitoring meteorological conditions and one-minute averaged TCl_g in outdoor air through HCl-TCl from July 7 to 11, 2022. Grey dashed line represents the background mixing ratio for $LLCl_g$.

3.5. HCl-TCl application to indoor cleaning

We applied a chlorine-based cleaning product four times in a well-lit indoor room and measured TCl_g using the HCl-TCl and HOCl analyzer during three of the cleaning events (Figure 6). One cleaning experiment was done without the HCl-TCl and had a maximum of 370 pptv HCl. These levels are comparable to peak HCl levels of ~500 pptv observed from surface application of bleach (Dawe et al., 2019). Consistent with previous speciated measurements (Mattila et al., 2020; Wong et al., 2017), HCl, HOCl, and TCl_g levels increased rapidly over ~5 minutes after the application of the cleaning product. The maximum levels of TCl_g from HCl-TCl during application 1, 2, and 3, were 49.2, 80.0, and 69.7 ppbv, respectively. The maximum levels of HOCl from

applications 1, 2, and 3, were 19.6, 24.2, and 16.8 ppbv, respectively, corresponding to 24 to 40 % of peak TCl_g and 14 to 22 % of integrated TCl_g. These TCl_g levels were several times higher than most observed in outdoor air (Section 3.4) and were within the range expected from previous experiments (Table S1). The levels of chlorinated species observed during bleaching events is variable, between 15 to 100s of ppbv (Mattila et al., 2020; Odabasi, 2008; Wang et al., 2019; Wong et al., 2017). By comparison, our highest observed mixing ratio was 80 ppbv. Because the multiphase chemical processes involved in bleach application are complex and poorly understood, it is difficult to compare levels between similar studies, given that the underlying ambient conditions can be very different. In addition, physical parameters, such as volume of cleaning solution applied, room size, and ventilation, can all affect observed mixing ratios. For example, studies have observed that gaseous NH_3 partitioning into aqueous bleach can produce large and variable amounts of chloramines, NH_2Cl, $NHCl_2$, and NCl_3 (Mattila et al., 2020; Wong et al., 2017). In our experiments, there was on average 82 ± 4 % of integrated TCl_g that could not be accounted for by the HOCl measurement. Additional chlorinated species that have previously been observed to be emitted from surface bleaching include $ClNO_2$, NH_2Cl, $NHCl_2$, NCl_3, and several chlorinated organics (Odabasi, 2008; Mattila et al., 2020; Wong et al., 2017) which likely also contributed to our measured TCl_g. We observed that TCl_g decayed ~15% faster than the air exchange rate (0.72 h^{-1}), indicating additional chemical loss pathways or surface interactions (Figure S6). We observed a shorter lifetime of HOCl relative to TCl_g, which is consistent with faster decay rates observed for HOCl and similar TCl_g species by Wong et. al., (2017). The HOCl started decreasing after ~300 s had elapsed while the TCl_g levels were still increasing. This suggests that reactions involving HOCl may have led to additional TCl_g species, which has been observed in laboratory studies (Wang et al., 2019).

In-situ measurements of TCl_g could provide additional insight into sources of chlorinated species to indoor environments by creating a total inventory from which the contributions of individual measured species can be compared and used to elucidate unknown TCl_g levels and mechanisms in real-time. Furthermore, several chlorinated species that have previously been observed to be emitted from surface bleaching, including Cl_2, HOCl, $ClNO_2$, NH_2Cl, $NHCl_2$, and NCl_3 (Mattila et al., 2020; Wong et al., 2017), have been measured by chemical ionization mass spectrometry (CIMS). Quantifying chlorinated species using CIMS remains challenging due to the required calibrations and difficulty in generating pure gas phase standards. It is therefore desirable to have a technique such as the one proposed in this study that does not require calibrations or knowledge of potential unknown TCl_g species. A combination of the two methods would help constrain the total levels while still observing speciation for key TCl_g species.

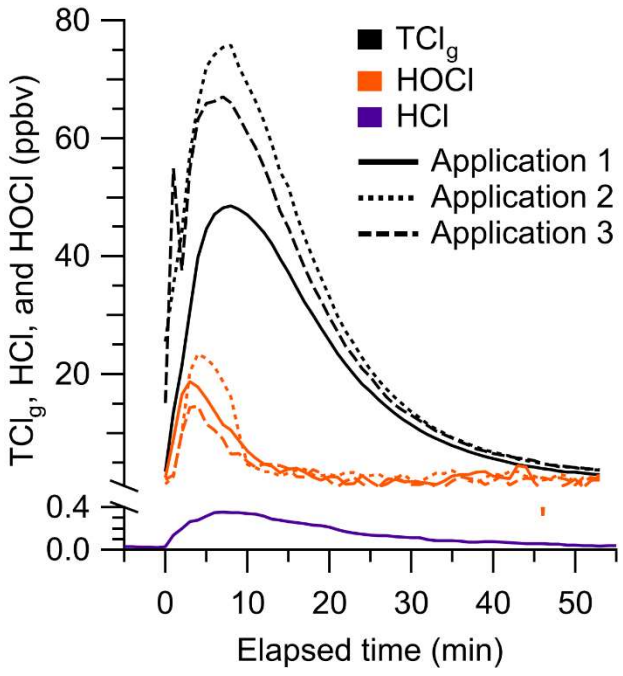

Figure 6. One-minute average HCl (purple), HOCl (orange), and TCl_g (black) observed during cleaning spray events. Mixing ratios were background corrected prior to each cleaning event. Each subsequent application of cleaner is illustrated by a lighter shade for HOCl and TCl_g.

4. Conclusions

In this work we developed, optimized, validated, and applied a method capable of converting TCl_g into gaseous HCl for detection by CRDS. Our TCl_g measurement technique, the HCl-TCl, is composed of a platinum catalyst mesh inside a quartz glass flow tube all contained within a split-tube furnace. The temperature and flow rate were optimized at 825 °C and 1.5 seconds, respectively using DCM. These conditions were validated by the complete conversion of organochlorine compounds with strong C-Cl bonds. The HCl-TCl was used to measure TCl_g outdoors, observing a range of 2.0 to 536.3 ppbv. Levels mostly exceeded the expected background mixing ratio of $LLCl_g$. We also applied the HCl-TCl to an indoor environment during commercial bleach spray cleaning events and observed varying increases in TCl_g (50–80 ppbv), which was in reasonable agreement with levels observed in previous speciated measurements. The agreement of HCl-TCl outdoor and indoor measurements with available bottom-up estimates indicates its efficacy under real-world scenarios. Rapid changes in TCl_g were observed in both outdoor and indoor environments indicating the utility of an in-situ technique to constrain the sources and chemistry of TCl_g, as well as its impact on air quality, climate, and health. We anticipate this approach could be used in several applications, including comparisons to speciated measurements of chlorinated compounds and to further explore Cl reactivity and cycling with respect for indoor and outdoor TCl_g.

Acknowledgements

We acknowledge the Sloan Foundation and Natural Sciences Engineering and Research Council of Canada for funding. We thank Melodie Lao and Yashar Iranpour for collecting air exchange rate data, Andrea Angelucci for collecting meteorological data, Dirk Verdoold for the custom

quartz tube, and Chris Caputo, John Liggio, Rob McLaren, and Trevor VandenBoer for helpful discussions. PME thanks the European Research Council. TFK is a Canada Research Chair in Environmental Analytical Chemistry. This work was undertaken, in part, thanks to funding from the Canada Research Chairs program.

Author contributions

TCF, RY, JS, and LRC collected and analyzed the data. TCF, RY, LRC, and CJY conceived of and designed the experiments with input from PME and TFK. Funding was obtained by TFK and CJY. The manuscript was written by TCF, RY, and CJY with input from all authors.

Data availability

Outdoor and indoor datasets can be found in Furlani et al. (2022, https://doi.org/10.20383/103.0649).

Competing interests

The authors declare no competing interests.

5. References

Adcock, K. E., Reeves, C. E., Gooch, L. J., Leedham Elvidge, E. C., Ashfold, M. J., Brenninkmeijer, C. A. M., Chou, C., Fraser, P. J., Langenfelds, R. L., Mohd Hanif, N., O'Doherty, S., Oram, D. E., Ou-Yang, C.-F., Phang, S. M., Samah, A. A., Röckmann, T., Sturges, W. T., and Laube, J. C.: Continued increase of CFC-113a (CCl3CF3) mixing ratios in the global atmosphere: emissions, occurrence and potential sources, Atmos. Chem. Phys., 18, 4737–4751, https://doi.org/10.5194/acp-18-4737-2018, 2018.

Andrews, S. J., Carpenter, L. J., Apel, E. C., Atlas, E., Donets, V., Hopkins, J. R., Hornbrook, R. S., Lewis, A. C., Lidster, R. T., Lueb, R., Minaeian, J., Navarro, M., Punjabi, S., Riemer, D., and Schauffler, S.: A comparison of very short lived halocarbon (VSLS) and DMS aircraft measurements in the tropical west Pacific from CAST, ATTREX and CONTRAST, Atmos. Meas. Tech., 9, 5213–5225, https://doi.org/10.5194/amt-9-5213-2016, 2016.

Berg, W. W., Crutzen, P. J., Grahek, F. E., Gitlin, S. N., and Sedlacek, W. A.: First measurements of total chlorine and bromine in the lower stratosphere, Geophys Res Lett, 7, 937–940, https://doi.org/https://doi.org/10.1029/GL007i011p00937, 1980.

Blankenship, A., Chang, D. P. Y., Jones, A. D., Kelly, P. B., Kennedy, I. M., Matsumura, F., Pasek, R., and Yang, G.: Toxic combustion by-products from the incineration of chlorinated hydrocarbons and plastics, Chemosphere, 28, 183–196, https://doi.org/https://doi.org/10.1016/0045-6535(94)90212-7, 1994.

Butz, A., Dinger, A. S., Bobrowski, N., Kostinek, J., Fieber, L., Fischerkeller, C., Giuffrida, G. B., Hase, F., Klappenbach, F., Kuhn, J., Lübcke, P., Tirpitz, L., and Tu, Q.: Remote sensing of volcanic CO_2, HF, HCl, SO_2, and BrO in the downwind plume of Mt. Etna, Atmos Meas Tech, 10, 1–14, https://doi.org/10.5194/amt-10-1-2017, 2017.

Dawe, K. E. R., Furlani, T. C., Kowal, S. F., Kahan, T. F., Vandenboer, T. C., and Young, C. J.: Formation and emission of hydrogen chloride in indoor air, Indoor Air, 70–78, https://doi.org/10.1111/ina.12509, 2019.

Doucette, W. J., Wetzel, T. A., Dettenmaier, E., and Gorder, K.: Emission rates of chlorinated volatile organics from new and used consumer products found during vapor intrusion investigations: Impact on indoor air concentrations, Environ Forensics, 19, 185–190, https://doi.org/10.1080/15275922.2018.1475433, 2018.

Fernando, S., Jobst, K. J., Taguchi, V. Y., Helm, P. A., Reiner, E. J., and McCarry, B. E.: Identification of the halogenated compounds resulting from the 1997 Plastimet Inc. fire in Hamilton, Ontario, using comprehensive two-dimensional gas chromatography and (ultra)high resolution mass spectrometry, Environ Sci Technol, 48, 10656–10663, https://doi.org/10.1021/es503428j, 2014.

Finlayson-Pitts, B. J.: Chlorine atoms as a potential tropospheric oxidant in the marine boundary layer, Research on Chemical Intermediates, 19, 235–249, https://doi.org/10.1163/156856793X00091, 1993.

Furlani, T., Ye, R., Stewart, J., Crilley, L., Edwards, P., Kahan, T., and Young, C.: Outdoor and indoor gaseous total chlorine measurement in Toronto Canada [data set], Federated Research Data Repository, https://doi.org/10.20383/103.0649, 2022.

Furlani, T. C., Veres, P. R., Dawe, K. E., Neuman, J. A., Brown, S. S., VandenBoer, T. C., and Young, C. J.: Validation of a new cavity ring-down spectrometer for measuring tropospheric gaseous hydrogen chloride., Atmos Meas Tech, 14, 5859–5871, https://doi.org/https://doi.org/10.5194/amt-2021-105, 2021.

Giardino, N. J. and Andelman, J. B.: Characterization of the emissions of trichloroethylene, chloroform, and 1,2-dibromo-3-chloropropane in a full-size, experimental shower., J Expo Anal Environ Epidemiol, 6, 413–423, 1996.

571 Hardy, J. E. and Knarr, J. J.: Technique for measuring the total concentration of gaseous fixed
572 nitrogen species, J Air Pollut Control Assoc, 32, 376–379,
573 https://doi.org/10.1080/00022470.1982.10465412, 1982.

574 Haskins, J. D., Jaeglé, L., Shah, V., Lee, B. H., Lopez-Hilfiker, F. D., Campuzano-Jost, P.,
575 Schroder, J. C., Day, D. A., Guo, H., Sullivan, A. P., Weber, R., Dibb, J., Campos, T., Jimenez,
576 J. L., Brown, S. S., and Thornton, J. A.: Wintertime gas-particle partitioning and speciation of
577 inorganic chlorine in the lower troposphere over the northeast United States and coastal ocean,
578 Journal of Geophysical Research: Atmospheres, 123, 12,897-12,916,
579 https://doi.org/10.1029/2018JD028786, 2018.

580 Henschler, D.: Toxicity of Chlorinated Organic Compounds: Effects of the introduction of
581 chlorine in organic Molecules, Angewandte Chemie International Edition in English, 33, 1920–
582 1935, https://doi.org/https://doi.org/10.1002/anie.199419201, 1994.

583 Kannan, K., Kawano, M., Kashima, Y., Matsui, M., and Giesy, J. P.: Extractable organohalogens
584 (EOX) in sediment and biota collected at an estuarine marsh near a former chloralkali facility,
585 Environ Sci Technol, 33, 1004–1008, https://doi.org/10.1021/es9811142, 1999.

586 Kato, M., Urano, K., and Tasaki, T.: Development of semi- and nonvolatile organic halogen as a
587 new hazardous index of flue gas, Environ Sci Technol, 34, 4071–4075,
588 https://doi.org/10.1021/es000881+, 2000.

589 Kawano, M., Falandysz, J., and Wakimoto, T.: Instrumental neutron activation analysis of
590 extractable organohalogens in the Antarctic Weddell seal (Leptonychotes weddelli), J
591 Radioanal Nucl Chem, 272, 501–504, https://doi.org/10.1007/s10967-007-0611-5, 2007.

592 Keene, William. C., Khalil, M. A. K., Erickson, David. J., McCulloch, A., Graedel, T. E., Lobert,
593 J. M., Aucott, M. L., Gong, S. L., Harper, D. B., Kleiman, G., Midgley, P., Moore, R. M.,
594 Seuzaret, C., Sturges, W. T., Benkovitz, C. M., Koropalov, V., Barrie, L. A., and Li, Y. F.:
595 Composite global emissions of reactive chlorine from anthropogenic and natural sources:
596 Reactive Chlorine Emissions Inventory, Journal of Geophysical Research: Atmospheres, 104,
597 8429–8440, https://doi.org/10.1029/1998JD100084, 1999.

598 Khalil, M. A. K., Moore, R. M., Harper, D. B., Lobert, J. M., Erickson, D. J., Koropalov, V.,
599 Sturges, W. T., and Keene, W. C.: Natural emissions of chlorine-containing gases: Reactive
600 Chlorine Emissions Inventory, Journal of Geophysical Research: Atmospheres, 104, 8333–8346,
601 https://doi.org/10.1029/1998JD100079, 1999.

602 Kolesar, K. R., Mattson, C. N., Peterson, P. K., May, N. W., Prendergast, R. K., and Pratt, K. A.:
603 Increases in wintertime $PM_{2.5}$ sodium and chloride linked to snowfall and road salt application,
604 Atmos Environ, 177, 195–202, https://doi.org/10.1016/j.atmosenv.2018.01.008, 2018.

605 Lao, M., Crilley, L. R., Salehpoor, L., Furlani, T. C., Bourgeois, I., Neuman, J. A., Rollins, A.
606 W., Veres, P. R., Washenfelder, R. A., Womack, C. C., Young, C. J., and VandenBoer, T. C.: A
607 portable, robust, stable and tunable calibration source for gas-phase nitrous acid (HONO), Atmos
608 Meas Tech, 13, 5873–5890, https://doi.org/10.5194/amt-13-5873-2020, 2020.

609 Lobert, J. M., Keene, W. C., Logan, J. A., and Yevich, R.: Global chlorine emissions from
610 biomass burning: Reactive Chlorine Emissions Inventory, Journal of Geophysical Research
611 Atmospheres, 104, 8373–8389, https://doi.org/10.1029/1998JD100077, 1999.

612 Maris, C., Chung, M. Y., Lueb, R., Krischke, U., Meller, R., Fox, M. J., and Paulson, S. E.:
613 Development of instrumentation for simultaneous analysis of total non-methane organic carbon
614 and volatile organic compounds in ambient air, Atmos Environ, 37, 149–158,
615 https://doi.org/https://doi.org/10.1016/S1352-2310(03)00387-X, 2003.

616 Massin, N., Bohadana, A. B., Wild, P., Héry, M., Toamain, J. P., and Hubert, G.: Respiratory
617 symptoms and bronchial responsiveness in lifeguards exposed to nitrogen trichloride in indoor
618 swimming pools., Occup Environ Med, 55, 258 LP – 263, https://doi.org/10.1136/oem.55.4.258,
619 1998.

620 Mattila, J. M., Lakey, P. S. J., Shiraiwa, M., Wang, C., Abbatt, J. P. D., Arata, C., Goldstein, A.
621 H., Ampollini, L., Katz, E. F., DeCarlo, P. F., Zhou, S., Kahan, T. F., Cardoso-Saldaña, F. J.,
622 Ruiz, L. H., Abeleira, A., Boedicker, E. K., Vance, M. E., and Farmer, D. K.: Multiphase
623 chemistry controls inorganic chlorinated and nitrogenated compounds in indoor air during bleach
624 cleaning, Environ Sci Technol, 54, 1730–1739, https://doi.org/10.1021/acs.est.9b05767, 2020.

625 Miyake, Y., Kato, M., and Urano, K.: A method for measuring semi- and non-volatile organic
626 halogens by combustion ion chromatography, J Chromatogr A, 1139, 63–69,
627 https://doi.org/https://doi.org/10.1016/j.chroma.2006.10.078, 2007a.

628 Miyake, Y., Yamashita, N., Rostkowski, P., So, M. K., Taniyasu, S., Lam, P. K. S., and Kannan,
629 K.: Determination of trace levels of total fluorine in water using combustion ion chromatography
630 for fluorine: A mass balance approach to determine individual perfluorinated chemicals in water,
631 J Chromatogr A, 1143, 98–104, https://doi.org/https://doi.org/10.1016/j.chroma.2006.12.071,
632 2007b.

633 Miyake, Y., Yamashita, N., So, M. K., Rostkowski, P., Taniyasu, S., Lam, P. K. S., and Kannan,
634 K.: Trace analysis of total fluorine in human blood using combustion ion chromatography for
635 fluorine: A mass balance approach for the determination of known and unknown organofluorine
636 compounds, J Chromatogr A, 1154, 214–221,
637 https://doi.org/https://doi.org/10.1016/j.chroma.2007.03.084, 2007c.

638 Montzka, S. A., Dutton, G. S., Portmann, R. W., Chipperfield, M. P., Davis, S., Feng, W.,
639 Manning, A. J., Ray, E., Rigby, M., Hall, B. D., Siso, C., Nance, J. D., Krummel, P. B., Mühle,
640 J., Young, D., O'Doherty, S., Salameh, P. K., Harth, C. M., Prinn, R. G., Weiss, R. F., Elkins, J.
641 W., Walter-Terrinoni, H., and Theodoridi, C.: A decline in global CFC-11 emissions during
642 2018−2019, Nature, 590, 428–432, https://doi.org/10.1038/s41586-021-03260-5, 2021.

643 Nuckols, J. R., Ashley, D. L., Lyu, C., Gordon, S. M., Hinckley, A. F., and Singer, P.: Influence
644 of tap water quality and household water use activities on indoor air and internal dose levels of
645 trihalomethanes, Environ Health Perspect, 113, 863–870, https://doi.org/10.1289/ehp.7141,
646 2005.

Odabasi, M.: Halogenated volatile organic compounds from the use of chlorine-bleach-containing household products, Environ Sci Technol, 42, 1445–1451, https://doi.org/10.1021/es702355u, 2008.

Odabasi, M., Elbir, T., Dumanoglu, Y., and Sofuoglu, S.: Halogenated volatile organic compounds in chlorine-bleach-containing household products and implications for their use, Atmos Environ, 92, 376–383, https://doi.org/10.1016/j.atmosenv.2014.04.049, 2014.

Pan, L. L., Atlas, E. L., Salawitch, R. J., Honomichl, S. B., Bresch, J. F., Randel, W. J., Apel, E. C., Hornbrook, R. S., Weinheimer, A. J., Anderson, D. C., Andrews, S. J., Baidar, S., Beaton, S. P., Campos, T. L., Carpenter, L. J., Chen, D., Dix, B., Donets, V., Hall, S. R., Hanisco, T. F., Homeyer, C. R., Huey, L. G., Jensen, J. B., Kaser, L., Kinnison, D. E., Koenig, T. K., Lamarque, J.-F., Liu, C., Luo, J., Luo, Z. J., Montzka, D. D., Nicely, J. M., Pierce, R. B., Riemer, D. D., Robinson, T., Romashkin, P., Saiz-Lopez, A., Schauffler, S., Shieh, O., Stell, M. H., Ullmann, K., Vaughan, G., Volkamer, R., and Wolfe, G.: The Convective Transport of Active Species in the Tropics (CONTRAST) experiment, Bull Am Meteorol Soc, 98, 106–128, https://doi.org/10.1175/BAMS-D-14-00272.1, 2017.

Prinn, R. G., Weiss, R. F., Arduini, J., Arnold, T., DeWitt, H. L., Fraser, P. J., Ganesan, A. L., Gasore, J., Harth, C. M., Hermansen, O., Kim, J., Krummel, P. B., Li, S., Loh, Z. M., Lunder, C. R., Maione, M., Manning, A. J., Miller, B. R., Mitrevski, B., Mühle, J., O'Doherty, S., Park, S., Reimann, S., Rigby, M., Saito, T., Salameh, P. K., Schmidt, R., Simmonds, P. G., Steele, L. P., Vollmer, M. K., Wang, R. H., Yao, B., Yokouchi, Y., Young, D., and Zhou, L.: History of chemically and radiatively important atmospheric gases from the Advanced Global Atmospheric Gases Experiment (AGAGE), Earth Syst. Sci. Data, 10, 985–1018, https://doi.org/10.5194/essd-10-985-2018, 2018.

Raff, J. D., Njegic, B., Chang, W. L., Gordon, M. S., Dabdub, D., Gerber, R. B., and Finlayson-Pitts, B. J.: Chlorine activation indoors and outdoors via surface-mediated reactions of nitrogen oxides with hydrogen chloride, Proceedings of the National Academy of Sciences, 106, 13647 LP – 13654, https://doi.org/10.1073/pnas.0904195106, 2009.

Riedel, T. P., Wolfe, G. M., Danas, K. T., Gilman, J. B., Kuster, W. C., Bon, D. M., Vlasenko, A., Li, S.-M., Williams, E. J., Lerner, B. M., Veres, P. R., Roberts, J. M., Holloway, J. S., Lefer, B., Brown, S. S., and Thornton, J. A.: An MCM modeling study of nitryl chloride ($ClNO_2$) impacts on oxidation, ozone production and nitrogen oxide partitioning in polluted continental outflow, Atmos. Chem. Phys., 14, 3789–3800, https://doi.org/10.5194/acp-14-3789-2014, 2014.

Roberts, J. M., Bertman, S. B., Jobson, T., Niki, H., and Tanner, R.: Measurement of total nonmethane organic carbon (C_y): Development and application at Chebogue Point, Nova Scotia, during the 1993 North Atlantic Regional Experiment campaign, Journal of Geophysical Research: Atmospheres, 103, 13581–13592, https://doi.org/https://doi.org/10.1029/97JD02240, 1998.

Saiz-Lopez, A. and Von Glasow, R.: Reactive halogen chemistry in the troposphere, Chem Soc Rev, 41, 6448–6472, https://doi.org/10.1039/c2cs35208g, 2012.

Schwartz-Narbonne, H., Wang, C., Zhou, S., Abbatt, J. P. D., and Faust, J.: Heterogeneous chlorination of squalene and oleic acid, Environ Sci Technol, 53, 1217–1224, https://doi.org/10.1021/acs.est.8b04248, 2019.

Shepherd, J. L., Corsi, R. L., and Kemp, J.: Chloroform in indoor air and wastewater: The role of residential washing machines., J Air Waste Manag Assoc, 46, 631–642, https://doi.org/10.1080/10473289.1996.10467497, 1996.

Sherwen, T., Schmidt, J. A., Evans, M. J., Carpenter, L. J., Großmann, K., Eastham, S. D., Jacob, D. J., Dix, B., Koenig, T. K., Sinreich, R., Ortega, I., Volkamer, R., Saiz-Lopez, A., Prados-Roman, C., Mahajan, A. S., and Ordóñez, C.: Global impacts of tropospheric halogens (Cl, Br, I) on oxidants and composition in GEOS-Chem, Atmos. Chem. Phys., 16, 12239–12271, https://doi.org/10.5194/acp-16-12239-2016, 2016.

Simpson, W. R., Brown, S. S., Saiz-Lopez, A., Thornton, J. A., and Von Glasow, R.: Tropospheric halogen chemistry: Sources, cycling, and impacts, Chem Rev, 115, 4035–4062, https://doi.org/10.1021/cr5006638, 2015.

Solomon, S.: Stratospheric ozone depletion: A review of concepts and history, Reviews of Geophysics, 37, 275–316, https://doi.org/10.1029/1999RG900008, 1999.

Stockwell, C. E., Kupc, A., Witkowski, B., Talukdar, R. K., Liu, Y., Selimovic, V., Zarzana, K. J., Sekimoto, K., Warneke, C., Washenfelder, R. A., Yokelson, R. J., Middlebrook, A. M., and Roberts, J. M.: Characterization of a catalyst-based conversion technique to measure total particulate nitrogen and organic carbon and comparison to a particle mass measurement instrument, Atmos. Meas. Tech., 11, 2749–2768, https://doi.org/10.5194/amt-11-2749-2018, 2018.

Unsal, V., Cicek, M., and Sabancilar, İ.: Toxicity of carbon tetrachloride, free radicals and role of antioxidants, Rev Environ Health, 36, 279–295, https://doi.org/doi:10.1515/reveh-2020-0048, 2021.

Veres, P., Gilman, J. B., Roberts, J. M., Kuster, W. C., Warneke, C., Burling, I. R., and de Gouw, J.: Development and validation of a portable gas phase standard generation and calibration system for volatile organic compounds, Atmos. Meas. Tech., 3, 683–691, https://doi.org/10.5194/amt-3-683-2010, 2010.

Wang, C., Collins, D. B., and Abbatt, J. P. D.: Indoor illumination of terpenes and bleach emissions leads to particle formation and growth, Environ Sci Technol, 53, 11792–11800, https://doi.org/10.1021/acs.est.9b04261, 2019.

White, C. W. and Martin, J. G.: Chlorine gas inhalation, Proc Am Thorac Soc, 7, 257–263, https://doi.org/10.1513/pats.201001-008SM, 2010.

WMO (World Meteorological Organization): Scientific Assessment of Ozone Depletion: 2018, Report No., Global Ozone Research and Monitoring Project, Geneva, Switzerland, 588 pp. pp., 2018.

Wong, J. P. S., Carslaw, N., Zhao, R., Zhou, S., and Abbatt, J. P. D.: Observations and impacts of bleach washing on indoor chlorine chemistry, Indoor Air, 27, 1082–1090, https://doi.org/10.1111/ina.12402, 2017.

Xu, D., Zhong, W., Deng, L., Chai, Z., and Mao, X.: Levels of extractable organohalogens in pine needles in China, Environ Sci Technol, 37, 1–6, https://doi.org/10.1021/es025799o, 2003.

Xu, D., Tian, Q., and Chai, Z.: Determination of extractable organohalogens in the atmosphere by instrumental neutron activation analysis, J Radioanal Nucl Chem, 270, 5–8, https://doi.org/10.1007/s10967-006-0302-7, 2006.

Xu, D., Dan, M., Song, Y., Chai, Z., and Zhuang, G.: Instrumental neutron activation analysis of extractable organohalogens in PM2.5 and PM10 in Beijing, China, J Radioanal Nucl Chem, 271, 115–118, https://doi.org/10.1007/s10967-007-0115-3, 2007.

Yang, M. and Fleming, Z. L.: Estimation of atmospheric total organic carbon (TOC) – paving the path towards carbon budget closure, Atmos Chem Phys, 19, 459–471, https://doi.org/10.5194/acp-19-459-2019, 2019.

Yeung, L. W. Y., Miyake, Y., Taniyasu, S., Wang, Y., Yu, H., So, M. K., Jiang, G., Wu, Y., Li, J., Giesy, J. P., Yamashita, N., and Lam, P. K. S.: Perfluorinated compounds and total and extractable organic fluorine in human blood samples from China, Environ Sci Technol, 42, 8140–8145, https://doi.org/10.1021/es800631n, 2008.

Young, C. J., Washenfelder, R. A., Edwards, P. M., Parrish, D. D., Gilman, J. B., Kuster, W. C., Mielke, L. H., Osthoff, H. D., Tsai, C., Pikelnaya, O., Stutz, J., Veres, P. R., Roberts, J. M., Griffith, S., Dusanter, S., Stevens, P. S., Flynn, J., Grossberg, N., Lefer, B., Holloway, J. S., Peischl, J., Ryerson, T. B., Atlas, E. L., Blake, D. R., and Brown, S. S.: Chlorine as a primary radical: Evaluation of methods to understand its role in initiation of oxidative cycles, Atmos Chem Phys, 14, 3427–3440, https://doi.org/10.5194/acp-14-3427-2014, 2014.

Zhai, S., Wang, X., McConnell, J. R., Geng, L., Cole-Dai, J., Sigl, M., Chellman, N., Sherwen, T., Pound, R., Fujita, K., Hattori, S., Moch, J. M., Zhu, L., Evans, M., Legrand, M., Liu, P., Pasteris, D., Chan, Y.-C., Murray, L. T., and Alexander, B.: Anthropogenic impacts on tropospheric reactive chlorine since the preindustrial, Geophys Res Lett, 48, e2021GL093808, https://doi.org/https://doi.org/10.1029/2021GL093808, 2021.

Zhang, W., Jiao, Y., Zhu, R., Rhew, R. C., Sun, B., and Dai, H.: Chloroform ($CHCl_3$) emissions from coastal Antarctic tundra, Geophys Res Lett, 48, e2021GL093811, https://doi.org/https://doi.org/10.1029/2021GL093811, 2021.